

# Poly(vinyl alcohol) Hydrogels with Broad-Range Tunable Mechanical Properties via the Hofmeister Effect

Shuwang Wu, Mutian Hua, Yousif Alsaïd, Yingjie Du, Yanfei Ma, Yusen Zhao, Chiao-Yueh Lo, Canran Wang, Dong Wu, Bowen Yao, Joseph Strzalka, Hua Zhou, Xinyuan Zhu,\* and Ximin He\*

Hydrogels, exhibiting wide applications in soft robotics, tissue engineering, implantable electronics, etc., often require sophisticatedly tailoring of the hydrogel mechanical properties to meet specific demands. For examples, soft robotics necessitates tough hydrogels; stem cell culturing demands various tissue-matching modulus; and neuron probes desire dynamically tunable modulus. Herein, a strategy to broadly alter the mechanical properties of hydrogels reversibly via tuning the aggregation states of the polymer chains by ions based on the Hofmeister effect is reported. An ultratough poly(vinyl alcohol) (PVA) hydrogel as an exemplary material (toughness  $150 \pm 20 \text{ MJ m}^{-3}$ ), which surpasses synthetic polymers like poly(dimethylsiloxane), synthetic rubber, and natural spider silk is fabricated. With various ions, the hydrogel's various mechanical properties are continuously and reversibly in situ modulated over a large window: tensile strength from  $50 \pm 9 \text{ kPa}$  to  $15 \pm 1 \text{ MPa}$ , toughness from  $0.0167 \pm 0.003$  to  $150 \pm 20 \text{ MJ m}^{-3}$ , elongation from  $300 \pm 100\%$  to  $2100 \pm 300\%$ , and modulus from  $24 \pm 2$  to  $2500 \pm 140 \text{ kPa}$ . Importantly, the ions serve as gelation triggers and property modulators only, not necessarily required to remain in the gel, maintaining the high biocompatibility of PVA without excess ions. This strategy, enabling high mechanical performance and broad dynamic tunability, presents a universal platform for broad applications from biomedicine to wearable electronics.

Hydrogels are 3D crosslinked polymeric materials with high water content. They have been widely studied because of their potential applications in various fields, such as tissue

engineering,<sup>[1]</sup> drug delivery,<sup>[2]</sup> implantable electronics,<sup>[3]</sup> energy storage devices,<sup>[4]</sup> coatings,<sup>[5]</sup> adhesives,<sup>[6]</sup> soft robotics,<sup>[7]</sup> etc. However, several issues persist and await solutions in bridging hydrogel researches and specific real-world applications. First, the high water content and loose crosslinking of hydrogels make them mechanically weak and often too fragile to handle practical tasks. Despite various advances in toughening hydrogels by forming double network,<sup>[8]</sup> adding nanofillers,<sup>[9]</sup> and mechanical training,<sup>[10]</sup> their mechanical performances are still less than satisfactory compared to waterless polymers.<sup>[11,12]</sup> Second, their resemblance to biological tissues make them the most ideal materials for tissue engineering.<sup>[13]</sup> In cell culturing, the elastic modulus of hydrogel should be on the same order of magnitude as that of the cells to promote adhesion between cells and hydrogel,<sup>[14]</sup> and to better mimic physiological conditions.

In stem cell studies, the modulus of hydrogels can also affect the differentiation,<sup>[15]</sup> proliferation,<sup>[16]</sup> mitigation,<sup>[17]</sup> and spreading<sup>[18]</sup> of stem cells. Therefore, tremendous effort has been spent on tuning the hydrogel modulus via testing the combinations of various composition,<sup>[19]</sup> concentration,<sup>[20]</sup> or curing conditions.<sup>[21]</sup> However, these approaches suffer from a narrow range of achievable modulus<sup>[22]</sup> or require sophisticated recipes.<sup>[19]</sup> Third, in some scenarios, dynamic or in situ tuning of the material between stiff and soft states is highly beneficial.<sup>[23,24]</sup> For instance, a neuron probe is desired to be initially rigid for easy insertion into brain tissue, but become soft subsequently to avoid causing damage or inflammation to adjacent neuron cells.<sup>[23,24]</sup> Some elastomers based on phase transition can exhibit a large range of tunable modulus, yet they are still not soft enough to match the modulus of neurons even at their softest states.<sup>[23]</sup> Compared to elastomers, hydrogels are more biocompatible. Additionally, water, ions, nutrition, and many other biologically relevant molecules can transport freely in the porous hydrogel matrix.<sup>[25]</sup> Despite these significant advantages, little research has focused on realizing dynamic in situ tuning of hydrogel mechanical properties, therefore limiting their applications in these important areas.

Dr. S. Wu, M. Hua, Y. Alsaïd, Y. Du, Y. Ma, Y. Zhao, C.-Y. Lo, C. Wang, D. Wu, Dr. B. Yao, Prof. X. He  
Department of Materials Science and Engineering  
University of California, Los Angeles  
Los Angeles, CA 90095, USA  
E-mail: ximinhe@ucla.edu

Dr. S. Wu, Dr. B. Yao, Prof. X. Zhu  
School of Chemistry and Chemical Engineering  
State Key Laboratory of Metal Matrix Composites  
Shanghai Jiao Tong University  
800 Dongchuan Road, Shanghai 200240, China  
E-mail: xyzhu@sjtu.edu.cn

Dr. J. Strzalka, Dr. H. Zhou  
X-Ray Science Division  
Argonne National Laboratory  
Argonne, IL 60439, USA

 The ORCID identification number(s) for the author(s) of this article can be found under <https://doi.org/10.1002/adma.202007829>.

DOI: 10.1002/adma.202007829

Different salts exhibit distinguishable abilities to precipitate proteins from aqueous solutions, which is known as the Hofmeister effect or ion-specific effect.<sup>[26]</sup> Such ion-specific phenomena have also been observed in other fields such as ice nucleation and recrystallization,<sup>[27]</sup> colloidal assembly,<sup>[28]</sup> and surface tension.<sup>[29]</sup> Regarding the synthetic macromolecules, plenty of researchers have studied the interactions among the ions, water molecules and polymer chains at the molecular level;<sup>[30]</sup> some works discussed how different ions affect the solubility and swelling of polymers;<sup>[31]</sup> a few papers reported improving hydrogel mechanical performance by soaking in salt solutions after the hydrogel is synthesized.<sup>[32,33]</sup> The previous studies of the ion-specific effect on hydrophilic polymers revealed that the ion-specific effects arise from the impacts of different ions on the hydration water around the hydrophilic functional groups on the hydrophobic chains.<sup>[34]</sup> However, the effects of different ions on the mechanical properties of hydrogels and utilizing the ion-specific effect to fabricate a functional hydrogel with variable mechanical properties have not yet been systematically studied.<sup>[32,33,35–37]</sup> Here, we proposed a freeze-soak method, soaking the frozen polymer solutions in the salt solutions, to fabricate hydrogels with different mechanical properties by tuning the aggregation of the hydrophilic polymer chains at the molecular level via the Hofmeister effect, to address the urgent demands of aforementioned various areas. Poly(vinyl alcohol) (PVA) was used as a model system here, because of the simple molecular structure of the amphiphilic macromolecule composed of a hydrophobic (CH<sub>2</sub>–CH<sub>2</sub>) backbone and hydrophilic (–OH) side-groups. Besides, it has many other outstanding merits such as biodegradability, biocompatibility, and nontoxicity<sup>[13]</sup> which have been well studied and made as hydrogels with various methods, such as freeze-thaw, chemically crosslinking, and mechanical training.<sup>[10,13]</sup> These make PVA an ideal exemplary polymer for the systematic study of the effects of various anions and cations on hydrogel networks, and to develop hydrogels with widely tunable mechanical, structural, and physical properties. In this study, by gelation of PVA in various salt solutions, we have fabricated an ultratough hydrogel (strain 2100 ± 300%, stress 15 ± 1 MPa, toughness, 150 ± 20 MJ m<sup>-3</sup>) which has larger strain and stress than the most tough hydrogels reported previously and is even tougher than the synthetic polymers like PDMS, synthetic rubber, and natural spider silk. Meanwhile we have realized the modulation of the hydrogel's mechanical properties over large windows: tensile strength ranging from 50 ± 9 kPa to 15 ± 1 MPa, toughness from 0.0167 ± 0.003 to 150 ± 20 MJ m<sup>-3</sup>, elongation from 300 ± 100% to 2100 ± 300%, and modulus from 24 ± 2 to 2500 ± 140 kPa. It is important to note that, during gelation the ions used only served to induce the aggregation of polymer chains and the formation of nano/microstructures. Instead of remaining in the polymer networks, the ions can be washed out completely and leave a hydrogel composed of pure PVA, hence maintaining the biocompatibility of the produced hydrogels without excess ions. Such a simple hydrogel, entirely physically assembled from PVA, hold important potential in broad applications in implantable tissues, cell culturing, stem cell differentiation, and neuron probes.

We first evaluated the effects of various ions on the gelation of PVA in their respective sodium and chloride salt solutions with the freeze-soak assay (Figure S1, Supporting Information). The 5 wt% PVA solution was first frozen at –20 °C, followed by the addition of 1.0 M salt solutions or pure water, after which the ice was allowed to melt at room temperature (Figure S1, Supporting Information). With freezing, the PVA was fixed in a specific shape macroscopically (Figure S2, Supporting Information) and the polymer chains were prepaced microscopically to facilitate the subsequent aggregation by ions to form a bulk hydrogel. The freezing also ensured clear judgement of whether the gelation happened during the thawing process. As shown in Figure S3 (Supporting Information), instead of forming a dense bulk hydrogel, the aggregates of PVA (without prior freezing) dispersed in the solution, presented a cloudy dispersion, when the solution state PVA was directly added into a salt solution (1.0 M Na<sub>2</sub>SO<sub>4</sub>). On the contrary, with freezing, a dense bulk hydrogel was formed (Figure S2, Supporting Information). This was attributed to the polymer chain prepacing, as they were squeezed between the growing ice crystals during the freezing process.<sup>[38]</sup> During the subsequent melting process, the gelation occurred in 1.0 M Na<sub>2</sub>SO<sub>4</sub> solution, which resulted in an opaque PVA hydrogel as shown in Figure S4 (Supporting Information); however, the PVA remained as a liquid solution when pure water or 1.0 M NaI solution was used (Figure S4, Supporting Information).

Generally, depending on the ion species, there are three kinds of possible interactions between the ions, the polymer chains, and the hydration water of polymer,<sup>[34,39]</sup> as illustrated by Figure 1a. First, some anions can polarize the hydration water molecules, which destabilizes the hydrogen bonds between the polymer and its hydration water molecules (Figure 1a<sub>1</sub>). Second, some ions can interfere with the hydrophobic hydration of the macromolecules by increasing the surface tension of the cavity surrounding the backbone (Figure 1a<sub>2</sub>). Third, other anions can bind directly and thus add extra charges to the PVA chains, which increase the solubility of the polymer (Figure 1a<sub>3</sub>). Specifically, ions such as SO<sub>4</sub><sup>2-</sup> and CO<sub>3</sub><sup>2-</sup> exhibit the first and second effects and could lead to the salting-out of polymers, thereby resulting in the collapse of polymer chains and forming small pores.<sup>[39]</sup> During the melting process of frozen samples in solutions of these ions, the water molecules were expelled from between the polymer chains, and the hydrogen bonds formed between the hydroxyl groups, which resulted in aggregation/crystallization of the polymer chains (Figure 1b). By contrast, other ions like NO<sub>3</sub><sup>-</sup> and I<sup>-</sup> exhibit the third interaction and lead to the salting-in of polymers.<sup>[39]</sup> As a result, the hydrogen bonds were dissociated, and the solubility increased when the frozen samples were melted in solutions of these other ions (Figure 1c).

To systematically investigate the effect of each type of anions/cations, series of sodium salts and chloride salts were chosen according to the Hofmeister series. As depicted in Figure 1d, when frozen samples were soaked in Na<sub>2</sub>SO<sub>4</sub> solution, PVA gelation occurred, as long as the ion concentration was higher than 0.5 M. However, in NaI solution, the PVA reverted to solution, even when the ion concentration was as high as 3.0 M. The critical gelation concentration of ions was also influenced by the concentration and molecular weight of PVA (Figure S5, Supporting

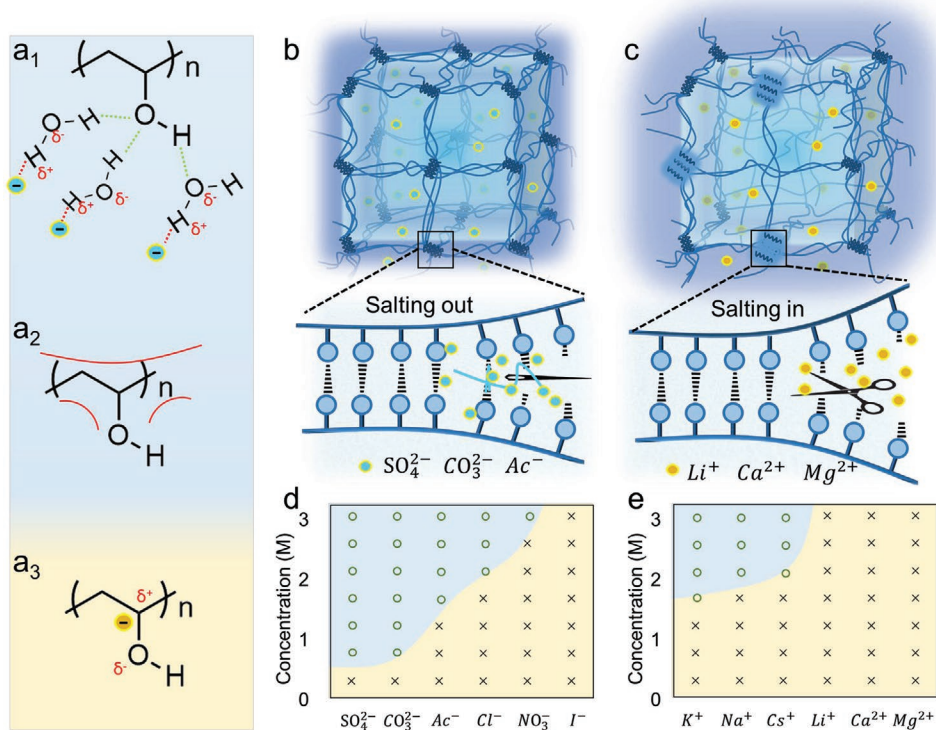


**Figure 1.** Schematics of the aggregation states of PVA polymer chains treated with different ions. a) The interactions among ions, polymer chains, and water molecules. b) Hydrogen bonds form between PVA polymer chains induced by ions due to salting-out effect. c) Hydrogen bonds break between PVA polymer chains induced by ions due to salting-in effect. d,e) Summary of the status of PVA gelation induced by different concentrations. The top-left region (blue) and the bottom-right region (yellow), respectively, represent the gelation and nongelation conditions.

Information). By comparing the critical gelation concentrations of 5 wt% PVA in different anions, a typical Hofmeister series emerged following the sequence  $\text{SO}_4^{2-} > \text{CO}_3^{2-} > \text{Ac}^- > \text{Cl}^- > \text{NO}_3^- > \text{I}^-$ , with  $\text{Na}^+$  as the constant counterion. The cations had similar specific effect on the gelation of PVA. However, the effect was less pronounced than that of anions, which was consistent with other phenomenon caused by the Hofmeister effect.<sup>[27]</sup> When  $\text{Cl}^-$  was used as the constant counterion, the critical gelation concentration of cations was 1.5 M at a minimum, and the PVA could not be gelled by  $\text{Li}^+$ ,  $\text{Ca}^{2+}$ , and  $\text{Mg}^{2+}$  (Figure 1e). The cation sequence based on critical PVA gelation concentration followed  $\text{K}^+ > \text{Na}^+ \approx \text{Cs}^+ > \text{Li}^+ \approx \text{Ca}^{2+} \approx \text{Mg}^{2+}$ . With systematic experiments, a chart of concentration versus ions was obtained as shown in Figure 1d,e, respectively, for anions and cations. In the chart, the blue and yellow regions represent the corresponding ions and their concentrations for gelation or nongelation, respectively.

The gelation occurred because of the salting-out effect, during which the aggregation of PVA chains were rearranged by ions. Therefore, this effect could be applied to tune the mechanical properties of the PVA hydrogels. To confirm this, PVA hydrogels made with 3 freeze-thaw cycles, after which the PVA solution became a translucent hydrogel (Figure S6, Supporting Information). Then the obtained hydrogels were soaked in 1.5 M  $\text{Na}_2\text{SO}_4$  for different times from 1 to 48 h (Figure S7, Supporting Information), which showed that after 24 h soaking, the mechanical performance reached a plateau. Afterward,

the mechanical properties of the PVA hydrogels soaked in different salt solutions for 24 h at room temperature were characterized systematically. Figure 2a,b showed the typical stress-strain curves of PVA hydrogels treated with different sodium salts and chloride salts chosen based on the Hofmeister series. Among the anion series, PVA hydrogel immersed in solution of  $\text{Na}_2\text{SO}_4$  had the largest ultimate stress (2.2 MPa) and strain (1400%), while the PVA hydrogel immersed in  $\text{I}^-$  had the smallest ultimate stress (50 kPa) and strain (300%) (Figure 2d). Systematically, the strength and toughness of PVA hydrogels of various anions followed the order:  $\text{SO}_4^{2-} > \text{CO}_3^{2-} > \text{Ac}^- > \text{Cl}^- > \text{NO}_3^- > \text{I}^-$ . Similar to the observations made with gelation process, the effects of cations were less pronounced than those of the anions. Here, the stress-strain curves of PVA hydrogels soaked in 3.0 M chloride salts were measured. As shown in Figure 2b,d, the PVA hydrogel of KCl gives the largest stress (1.1 MPa) as the hydrogel was stretched to 700%. At the same time, the stress of PVA hydrogel immersed in LiCl was only 100 kPa as the hydrogel was stretched to 300% (Figure 2b,d). Note that the stress-strain curves of gels treated by  $\text{Ca}^{2+}$  and  $\text{Mg}^{2+}$  could not be measured because the PVA hydrogel almost dissolved in these salt solutions. By comparing the strength and toughness, a cation series was obtained:  $\text{K}^+ > \text{Na}^+ \approx \text{Cs}^+ > \text{Li}^+ > \text{Ca}^{2+} \approx \text{Mg}^{2+}$ . To study the stability of the mechanical properties of PVA hydrogels in pure water for a long period of time, the salts were washed out with abundant pure water and the hydrogels were soaked in pure water for more than 48 h. As

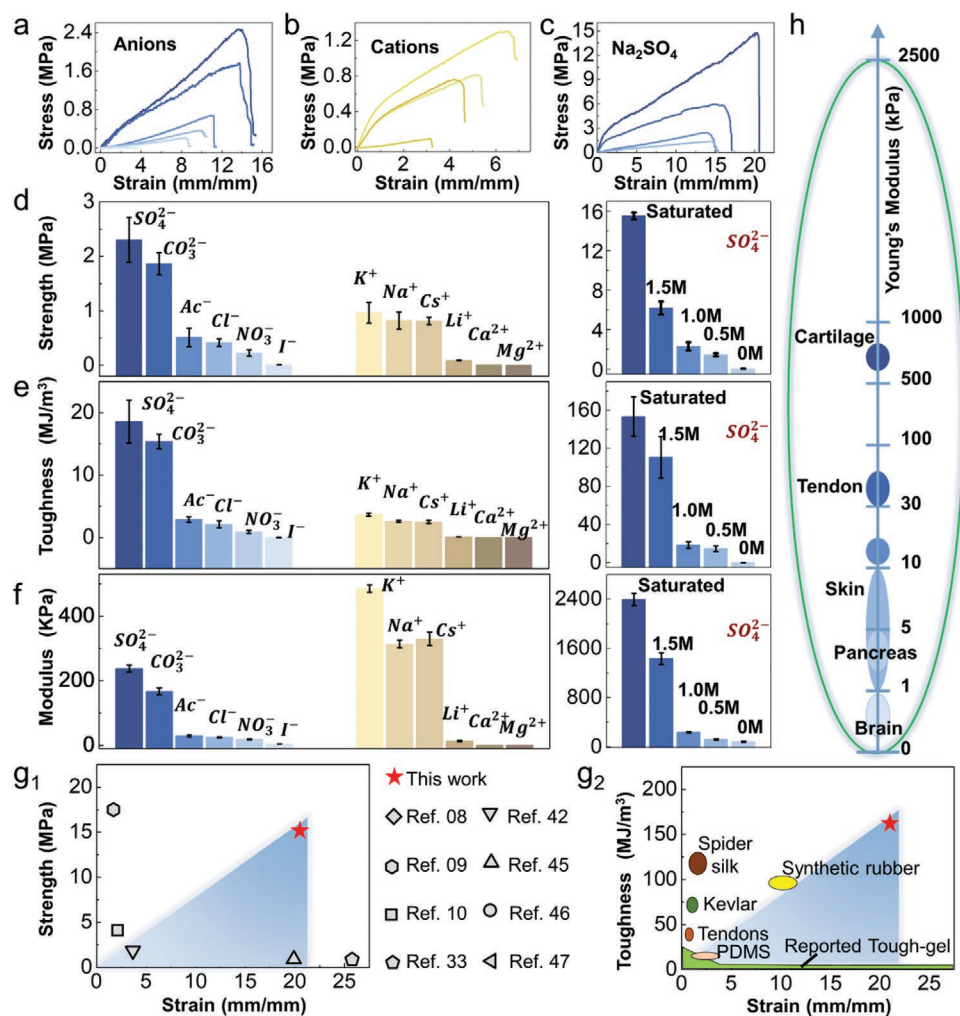


**Figure 2.** Tunable mechanical properties of PVA hydrogels by various ions. a–c) Representative stress–strain curves of PVA hydrogels soaked in 1 M sodium salts (a), 3 M chloride salts (b), and Na<sub>2</sub>SO<sub>4</sub> with concentration range from 0 M to saturated (c). d–f) Strengths (d), toughness (e), and moduli (f) of PVA hydrogels tuned by various anions (with Na<sup>+</sup> as the constant counterion); different cations (with Cl<sup>-</sup> as the constant counterion); and Na<sub>2</sub>SO<sub>4</sub> with concentrations ranging from 0 M to saturated. g) Diagrams of ultimate strength versus ultimate strain (g<sub>1</sub>), and toughness versus ultimate strain (g<sub>2</sub>) of the hydrogels treated with different ions compared with other tough hydrogels and polymers reported in references. h) The moduli ranges of soft tissues in the human body and the PVA hydrogels regulated by ions with different concentrations. The green circle in (h) refers to the moduli range of the as-prepared PVA hydrogels. The blue shaded areas in (g<sub>1</sub>) and (g<sub>2</sub>) indicate the ranges of strength and toughness that can be tuned via the Hofmeister effect.

shown in Figure S8 (Supporting Information), their mechanical properties showed decreases, yet significantly higher than that of the untreated PVA hydrogel prepared by 3 cycles of freeze-thaw only, which was too soft to be measured. Particularly, the hydrogel made in the saturated Na<sub>2</sub>SO<sub>4</sub> solution had a strength around 6.3 MPa with an elongation around 1900% after removing the salts in the hydrogel and soaking in pure water for 48 h. Additionally, the strength retention increased as the salt concentration decreased (Figure S8,e,f, Supporting Information). The images showed that the hydrogel remained unchanged even after immersion in water for three months (Figure S9, Supporting Information). This confirmed that during the salting-out process, the ions mainly induced the aggregation of the polymer chains, but did not serve as components in the aggregated hydrogel.<sup>[40]</sup> Moreover, the viscoelastic behaviors of the hydrogels were measured after washing out the salts. As shown in Figure S10 (Supporting Information), the

storage moduli and loss moduli of hydrogels follow the same order of ions. The hydrogels showed mainly an elastic behavior, as the storage moduli were an order of magnitude higher than loss moduli.

Furthermore, the specific ion effect is usually concentration sensitive. Here, Na<sub>2</sub>SO<sub>4</sub> was used as an example to study the influence of concentrations. As concentration of Na<sub>2</sub>SO<sub>4</sub> increased from 0.5 M to saturated (≈1.8 M at room temperature), the ultimate stress and maximum strain of the resulted hydrogel increased significantly from 1.0 to 15.0 MPa and from 1500% to 2100%, respectively (Figure 2c). Toughness and modulus exhibited similar trends, which increased from 3.1 to 153.41 MJ m<sup>-3</sup> and from 24 to 2500 kPa, respectively (Figure 2d,e,f). Note that the hydrogel soaked with saturated Na<sub>2</sub>SO<sub>4</sub> showed higher ultimate stress and strain that surpassed the values reported in previous works studying tough hydrogels (Figure 2g<sub>1</sub>) by 10 to 10<sup>3</sup> fold,<sup>[41–43]</sup> and the corresponding toughness

was larger than the water-free polymers like PDMS, synthetic rubber and natural spider silk (Figure 2g<sub>2</sub>). Furthermore, via changing the ions or concentrations, the modulus of PVA hydrogels can be easily tuned within a broad range, from near 24 to 2500 kPa, which covered all the moduli of soft tissues in the human body<sup>[38,44]</sup> as shown in Figure 2h. With such a large range of moduli and biocompatibility, the PVA hydrogels can offer a very promising material platform for stem cells to differentiate into various functional cells, ranging from extremely soft brain cells to very rigid cartilage cells. This strategy was also applicable to other polymers such as gelatin (Figure S11, Supporting Information). Additionally, in contrast to traditional hydrogels with certain mechanical properties achieved by ionic crosslinking,<sup>[45,46]</sup> the ions used here, functioned as a gelation trigger rather than the components of the hydrogels, which was washed out with DI water and left the final hydrogel structure ion-free without altering its properties or comprising the biocompatibility.

Along with the tunable mechanical properties over large ranges, the water contents remained high, with slight differences among the PVA hydrogels soaked in different ions solutions. As shown in Figure S12 (Supporting Information), the water contents of PVA hydrogels treated with various sodium salts followed the order:  $\text{Na}_2\text{SO}_4 < \text{Na}_2\text{CO}_3 < \text{NaAc} < \text{NaCl} < \text{NaNO}_3 < \text{NaI}$ . X-ray diffraction (XRD) was used to characterize the crystalline domains of the PVA hydrogels. As shown in Figure 3a; and Figure S13 (Supporting Information), after soaking in 1 M  $\text{Na}_2\text{SO}_4$ , there were obvious crystalline aggregates in the hydrogel which yielded the opaque appearance of

the hydrogel via scattering of light. PVA hydrogel soaked in  $\text{NaNO}_3$  (termed as PVA- $\text{NO}_3$ ) had no apparent crystalline peaks (Figure 3b), therefore was translucent. Hence, judging from the XRD diffraction and the opacity of PVA hydrogel soaked with  $\text{Na}_2\text{SO}_4$  (termed as PVA- $\text{SO}_4$ ), there were crystalline domains dispersed between random coil chains in the PVA hydrogel as shown in the schematic in Figure 1b. However, there were few crystalline aggregates in the PVA- $\text{NaNO}_3$  (Figure 1c). The impacts of different salts on the crystallization of PVA were further confirmed with DSC as shown in Figure S14 (Supporting Information). The crystallinities of the hydrogels treated with various sodium salts followed the order:  $\text{Na}_2\text{SO}_4 > \text{Na}_2\text{CO}_3 > \text{NaNO}_3 \approx \text{NaI}$ . Figure 3c,d; and Figure S15 (Supporting Information) showed the morphologies of PVA- $\text{SO}_4$  and PVA- $\text{NO}_3$ . The PVA- $\text{SO}_4$  hydrogel had the highest pore density and the smallest pore size of around 200 nm among all tested ions of the same concentration (Figure 3c; and Figure S15, Supporting Information). Its structure presented continuous networks of nanofibrils. By contrast, in PVA- $\text{NO}_3$  hydrogel, most pores were around 2  $\mu\text{m}$  in size, with a few smaller pores on the walls of the larger pores (Figure 3d). Such a significant difference in morphology between PVA- $\text{SO}_4$  and PVA- $\text{NO}_3$  was believed to originate from the aforementioned specific ion effect. Ions such as  $\text{SO}_4^{2-}$  and  $\text{CO}_3^{2-}$  triggered the salting-out of the polymers, thereby resulting in the spontaneous collapse of polymer chains and formation of the small pores. Ions like  $\text{NO}_3^-$  and  $\text{I}^-$  led to the salting-in of the polymer, which resulted in partial dissolution of the polymer, and has led to larger pores (Figures S15 and S16, Supporting Information).

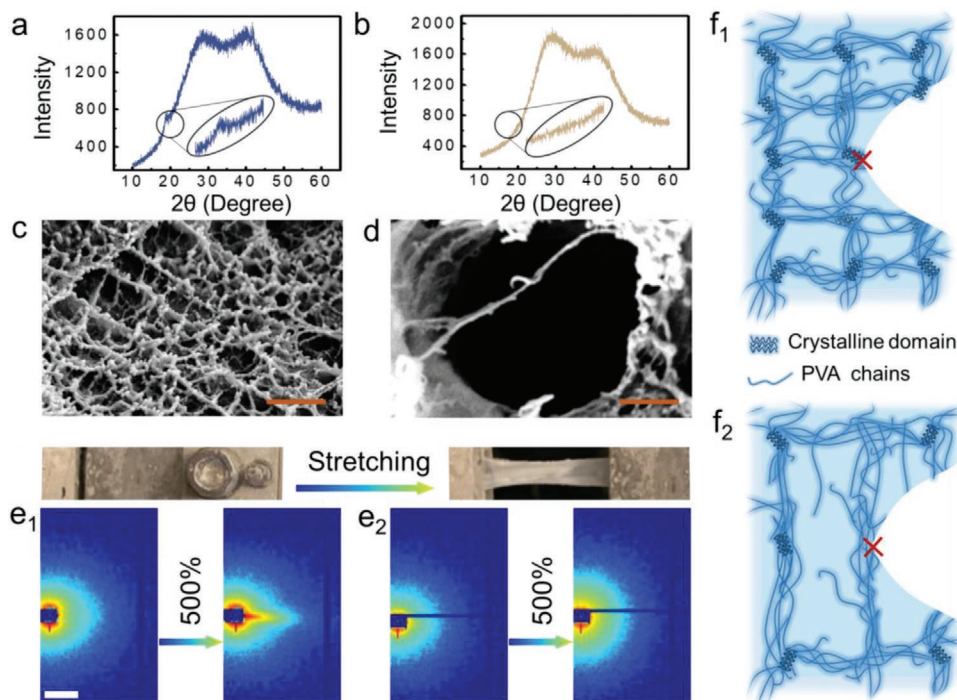


**Figure 3.** Characterizations of PVA hydrogels soaked in 1 M  $\text{Na}_2\text{SO}_4$  and  $\text{NaNO}_3$ . a,b) XRD spectra of PVA hydrogels soaked with 1.0 M  $\text{Na}_2\text{SO}_4$  and  $\text{NaNO}_3$ . The inset shows the enlarged spectra to compare the crystalline information. c,d) SEM images of PVA- $\text{SO}_4$  and PVA- $\text{NO}_3$ . SEM scale bars 500 nm. e) SAXS patterns of PVA- $\text{SO}_4$  and PVA- $\text{NO}_3$  during tensile loading. SAXS scale bar 0.025  $\text{\AA}^{-1}$ . f) The schematic structures of PVA- $\text{SO}_4$  and PVA- $\text{NO}_3$ , with different densities of nanofibrils and crystalline domains and thus different crack blunting and pinning effects.

For PVA-SO<sub>4</sub> during stretching, the nanofibril spacing decreased significantly as the network became partially aligned, as indicated by the stretch of SAXS pattern perpendicular to the stretching direction (Figure 3e1). The average nanofibril spacing decreased from ~90 to ~30 nm (Figure S17, Supporting Information) when the strain increased from 0% to 500%. Such scattering difference was not observed for PVA-NO<sub>3</sub>, which had no structural features of the same length scale (Figure 3e<sub>2</sub>). From a fracture mechanics perspective, there were three reasons why the PVA-SO<sub>4</sub> was much tougher than the PVA-NO<sub>3</sub>. First, because of the two opposite effects, salting-out and salting-in, the density of polymer chains in PVA-SO<sub>4</sub> was higher than that in PVA-NO<sub>3</sub> (also verified by the different water contents in these two hydrogels as shown in Figure S12, Supporting Information). Second, during the salting-out process, abundant hydrogen bonds were formed which resulted in strong aggregation and partial crystallization of the polymer chains (Figures 1b and 3a), while PVA-NO<sub>3</sub> went through a reverse process of salting-in (Figures 1c and 3b). Therefore, the density of crystalline domains in PVA-SO<sub>4</sub> was much higher than that in PVA-NO<sub>3</sub>. The structures and material elasticity were strengthened and improved by the crystalline domains

which acted as rigid high functionality cross-linkers.<sup>[11]</sup> Meanwhile, the crystalline domains delayed the fracture of individual nanofibrils by crack pinning leading to the toughness enhancement<sup>[10]</sup> (Figure 3f). Third, compared to PVA-NO<sub>3</sub> which has no nanofibril features, when PVA-SO<sub>4</sub> was stretched, the decrease in interfibril spacing led to an increase in concentration of nanofibrils per unit cross-section, which in situ strengthened the material (Figure 3e). In short, PVA-SO<sub>4</sub> obtained extraordinary toughness and largest ranges of strength and moduli because of the densification enhancements on three levels: polymer chains, crystalline domains, and nanofibrils (Figure 3).

The mechanical properties of PVA hydrogel can be altered by different ions dynamically which means the tough gel made by some salting-out salts can be softened by some salting-in salts. As illustrated in Figure 4a after soaking in saturated Na<sub>2</sub>SO<sub>4</sub> and washed with excess water, the PVA hydrogel became opaque and shrunk slightly. Subsequently, the opaque PVA hydrogel was soaked in 3 M CaCl<sub>2</sub> for 48 h, where it transformed into a translucent hydrogel that swelled back slightly. Meanwhile, the corresponding strength, toughness, and modulus were tuned dynamically from 15.53 MPa, 153.41 MJ m<sup>-3</sup> and 2500 kPa to 0.09 MPa, 2.48 MJ m<sup>-3</sup>, and 34 kPa, respectively. Many

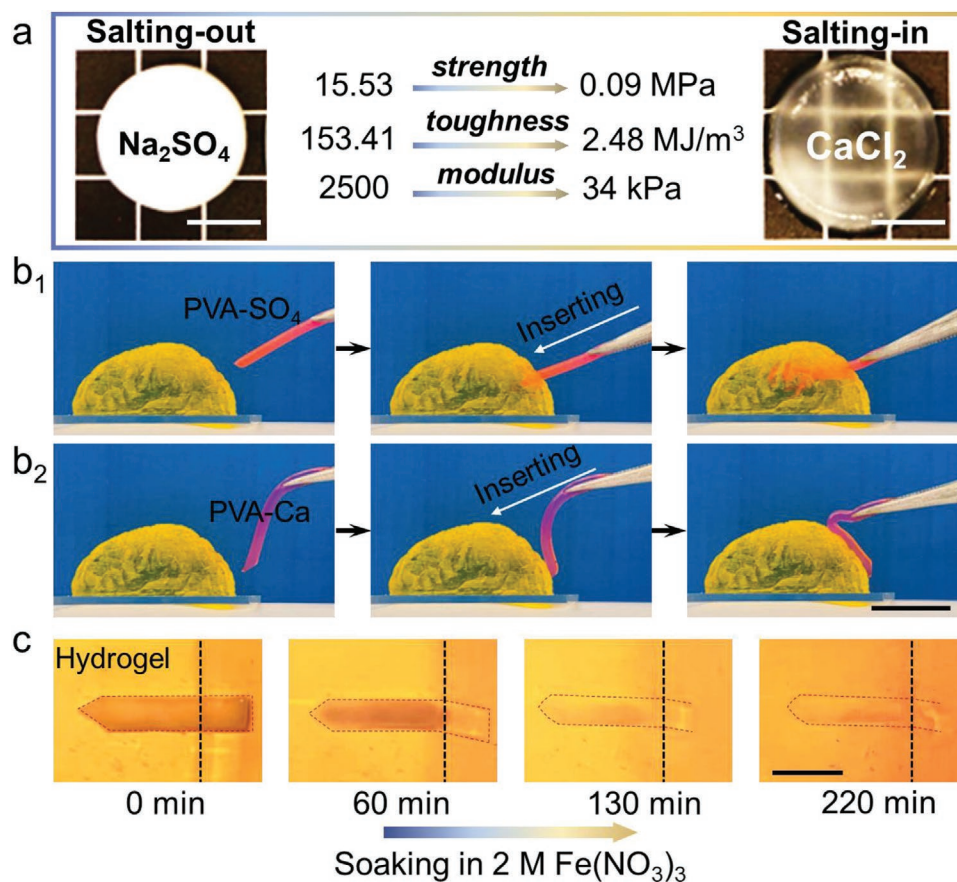


**Figure 4.** PVA hydrogel softened or toughened by Na<sub>2</sub>SO<sub>4</sub> and CaCl<sub>2</sub>, respectively. a) Optical images of PVA hydrogel after soaking with solutions of saturated Na<sub>2</sub>SO<sub>4</sub> and 3 M CaCl<sub>2</sub>. The PVA hydrogel was toughened by Na<sub>2</sub>SO<sub>4</sub> and then softened by CaCl<sub>2</sub>, with the corresponding values of strength, toughness, and modulus listed. Scale bar = 1 cm. b<sub>1</sub>) A stiff PVA hydrogel toughened by 1 M Na<sub>2</sub>SO<sub>4</sub> penetrating into a soft brain-tissue-mimicking hydrogel. b<sub>2</sub>) A soft PVA hydrogel treated with 1 M CaCl<sub>2</sub> could not penetrate the same brain-tissue-mimicking hydrogel. The hydrogel probes were dyed with Rhodamine B for visualization. c) The hydrogel probe inserted in the brain-mimic hydrogel was soaked in a 2 M Fe(NO<sub>3</sub>)<sub>3</sub> solution. Over 220 min, the original white hydrogel probe gradually became translucent. Scale bars of (b) and (c) are 1 cm and 1 mm, respectively.

salting-out salts have been tested, such as  $\text{LaCl}_3$ ,  $\text{Al}(\text{NO}_3)_3$  and  $\text{Fe}(\text{NO}_3)_3$  (Figure S18, Supporting Information), and  $\text{Fe}(\text{NO}_3)_3$  was found to have the strongest salting-in effect, which can soften the tough hydrogels rapidly. As shown in Movie S1 (Supporting Information), the hydrogel became transparent and soft in less than 10 min in the 3 M  $\text{Fe}(\text{NO}_3)_3$ . It took 26 and 100 min, respectively, to soften the PVA hydrogel in 2 and 1 M solutions (Figure S19, Supporting Information). The effect of repeated soaking in salting-in and salting-out solutions on the mechanical performances were also studied. As shown in Figure S20 (Supporting Information), after the first cycle, the strength can be recovered to 72% and 48% for the second cycle. As the cycles increased further, the strength decreased at a slower rate. The decrease of mechanical property was mainly attributed to that polymers partially dissolved away from the bulk material during soaking in the salting-in solution. Such hydrogel with variable mechanics can be potentially used as neuron probes, which need to be rigid initially to easily insert into brain tissue, and as soon as after insertion, become softened subsequently to match the modulus of neuron cells<sup>[3]</sup> ( $\approx 10$  kPa). Here, to mimic the brain tissue, a soft hydrogel made of polyacrylamide with a brain-tissue-matching modulus ( $\approx 10$  kPa) was utilized. When the PVA hydrogel probe was toughened by  $\text{Na}_2\text{SO}_4$ , it could penetrate the soft polyacrylamide hydrogel as shown in Figure 4b<sub>1</sub>, while the soft PVA hydrogel soaked in 1 M  $\text{CaCl}_2$  could not (Figure 4b<sub>2</sub>, and Figure S21, Supporting Information). Furthermore, to demonstrate on-site stiffness tuning, i.e., the hydrogel can be softened after “implantation,” the hydrogel probe inserted in the brain-mimicking hydrogel was soaked in a 2 M  $\text{Fe}(\text{NO}_3)_3$  solution. As shown in Figure 4c the originally white hydrogel probe became translucent gradually over 220 min of soaking, indicating that the PVA hydrogel probe can be in situ softened by ions even, while constrained inside another matrix. This on-site stiffness tunability presents attractive advantages and opportunities for applications that require local tuning of material properties, unachievable with conventional materials whose properties are set once produced or can be tuned only with extreme conditions, such as high temperature.<sup>[23]</sup>

In summary, with a freeze-soak method, it was discovered that ions have a specific effect on the gelation of PVA. The effects of different ions on the ion-facilitated gelation and the toughening of PVA followed such orders:  $\text{SO}_4^{2-} > \text{CO}_3^{2-} > \text{Ac}^- > \text{Cl}^- > \text{NO}_3^- > \text{I}^-$  for anions and  $\text{K}^+ > \text{Na}^+ \approx \text{Cs}^+ > \text{Li}^+ \approx \text{Ca}^{2+} \approx \text{Mg}^{2+}$  for cations. The ion-specific gelation originated from the different interaction modes with PVA polymer chains that resulted in either salting-out or salting-in. The PVA hydrogels showed mechanical properties that followed the Hofmeister series after being treated with various salts solutions. In addition to the different types of ions used, higher salt concentration also enhanced their influence on the mechanical properties of the produced hydrogels. Therefore, by changing the types and concentrations of salts, the mechanical properties of PVA hydrogels could be tuned with a large window. Specifically, the tensile strength was tuned from  $50 \pm 9$  kPa to  $15 \pm 1$  MPa, toughness was regulated from  $0.0167 \pm 0.003$  to  $150 \pm 20$  MJ  $\text{m}^{-3}$ , and the elongation varied from  $300 \pm 100\%$  to  $2100 \pm 300\%$ . Specially, the PVA hydrogel treated with saturated  $\text{Na}_2\text{SO}_4$  solution showed the largest strength ( $15 \pm 1$  MPa), toughness ( $150 \pm 20$  MJ  $\text{m}^{-3}$ ), and elongation ( $2100 \pm 300\%$ ),

which can be considered as an ultratough and highly-stretchable hydrogel. The hydrogel soaked with saturated  $\text{Na}_2\text{SO}_4$  showed higher ultimate stress and strain surpassing the values reported in previous works of tough hydrogels by  $10\text{--}10^3$  fold, and the toughness of hydrogels soaked with saturated  $\text{Na}_2\text{SO}_4$  is higher than that of water-free polymers like PDMS, synthetic rubber and natural spider silk. The hydrogels treated with different salts showed significantly different mechanical properties, which resulted from the various degrees of aggregation of polymers chains because of the specific interactions among the ions, water molecules, and polymer chains at the molecular level. In this study, PVA was used as an exemplary polymer to demonstrate the regulation of mechanical properties by tuning the aggregation states of polymer chains. Since the classic Hofmeister effect is universal for hydrophilic polymers, the presented strategy can be extended to many other systems composed of hydrophilic polymers.

Furthermore, the demonstration of onsite dynamically tunable stiffness presented a potentially new strategy to design hydrogel-based neuron probes with the stiffness tuned by ions. Although currently the salt concentration used in the proof of concept here is higher than that in human body, through optimization the hydrogel neuron probe may be further improved for practical applications. Additionally, the ions utilized for fabricating the hydrogels only induced the aggregation of polymer chains and the formation of structures, instead of serving as the components of hydrogels. Hence, after soaking treatment in ions solutions and subsequently washing out the ions completely, the final ion-free PVA hydrogels could well maintain their properties and the highly desirable biocompatibility without interferences from potentially hazardous ions used when making the hydrogels. With this facile method and the excellent in situ and broad-range tunability of mechanical properties, PVA hydrogels can be expanded to a broader-based platform to meet the needs of a variety of areas ranging from biomedicine to robotics and wearable electronics.

## Experimental Section

**Materials:** Poly(vinyl alcohol) (PVA) (weight-average molecular weight ( $M_w$ ) of 89–98 kDa; degree of hydrolysis of 99%; Sigma-Aldrich), glutaraldehyde (25 v%; Sigma-Aldrich), hydrochloric acid (36.5–38 wt %, Sigma-Aldrich), salts (analytical grade; Sigma-Aldrich) Rhodamine B, acrylamide (analytical grade; Sigma-Aldrich), *N,N'*-methylenebisacrylamide, and 2-hydroxy-2-methylpropiophenone were used as received.

**Preparation of PVA and Salt Solutions:** 2, 5, and 10 wt% PVA solutions were prepared by dissolving PVA powder in deionized (DI) water under vigorous stirring and heating (95 °C). After degassing by sonication for 1 h, clear solutions were obtained. Various salt solutions of different concentrations were prepared by dissolving salts in DI water. After sonication for 10 min, clear salt solutions were obtained.

**Fabrication of Hydrogel:** To judge if the PVA solutions can form hydrogels, 1.5 mL PVA solution of 5 wt% was injected into a vial and was frozen at  $-20$  °C. Then the frozen samples were transferred to room temperature and different salt solutions of 1.0 M or DI water were added, where the ice melted over time. After 1 h, the vial was shaken to see if the solution became a hydrogel. To fabricate the hydrogels for measuring the mechanics, 20 mL 10 wt% PVA solution was poured into a Petri dish and freeze–thawed for 3 cycles, after which it became a hydrogel. The hydrogel was cut into strips of 5 mm  $\times$  3 cm and soaked into different salt solutions

with specific concentrations for 24 h. To test the stability of hydrogels soaking in pure water for a long period of time, the hydrogels were first freeze–thawed for three cycles and then soaked in solutions of different concentrations from 0.5 M to saturate. Afterward, the samples were soaked in a large container (volume = 6000 mL) for 2 days, during which the water was exchanged for 4 times. The mechanical properties of hydrogels were measured after the thorough washing and swelling. The PVA hydrogels with different shapes were obtained by freezing the PVA solutions in specific molds, followed by soaking in 1.5 M Na<sub>2</sub>SO<sub>4</sub>. At last, the molds were removed. To make gelatin hydrogels, a solution of 10 wt% gelatin was prepared by dissolving 10 g gelatin in 90 mL pure water at 50 °C with stirring. Afterward, the solution was poured in a petri dish and kept at room temperature overnight for gelation. At last, the gelatin hydrogels were soaked in various 1 M salt solutions for 24 h and characterized.

**Tensile Testing:** Hydrogels were cut into dog-bone shaped specimens with gauge width of 2 mm for regular tensile testing. The thickness of each specimens was measured with a caliper. The force–displacement data were obtained using a Cellscale Univert mechanical tester with a 50N loading cell installed. The stress–strain curves were obtained by division of an initial gauge cross-section area and an initial clamp distance.

**SEM Characterization:** For the characterization of the micro- and nanostructures of the hierarchically aligned hydrogels, all hydrogel samples were immersed in DI water for 24 h before freeze drying using a Labconco FreeZone freeze drier. The freeze-dried hydrogels were cut along the aligned direction to expose the inside and sputtered with gold before carrying out the imaging using a ZEISS Supra 40VP SEM.

**X-Ray Scattering Characterization:** The hydrogels treated with different ions were cut into 1 cm by 4 cm rectangles and washed with plenty of DI water for before testing. The beamline station used was APS 8-ID-E (Argonne National Laboratory) equipped with Pilatus 1 M detector. A customized linear stretcher was used to hold the samples and stretch on demand for in situ X-ray scattering measurements. A MATLAB toolbox “GXSGUI” was used for further line-cut analysis and space conversion of the obtained scattering pattern.<sup>[47]</sup>

**Water Content Measurement:** The hydrogels were washed with plenty of pure water after soaking in different salt solutions for 24 h (concentration: 1.5 M). The water contents of the PVA hydrogels were measured by comparing the weights before and after freeze-drying. Excess surface water was wiped away from the hydrogel surface before measuring the weight ( $m_w$ ). The hydrogel samples were instantly frozen in liquid nitrogen and freeze-dried with a Labconco FreeZone freeze drier. Weight before ( $m_w$ ) and after freeze drying ( $m_d$ ) were measured with a balance. The water content was calculated by  $(m_w - m_d) / m_w * 100\%$ .

**Measurement of Crystallinity:** The crystallinities of PVA–SO<sub>4</sub> and PVA–NO<sub>3</sub> were measured by DSC (DSC-Q8000). The PVA–SO<sub>4</sub> and PVA–NO<sub>3</sub> were first soaked in the 100 mL solution consisting 20 mL of glutaraldehyde and 1 mL of hydrochloric acid for 6 h. During this process, the amorphous parts in the hydrogels were crosslinked and fixed by glutaraldehyde. Thereafter, the samples were immersed in DI water for 24 h to remove the unreacted glutaraldehyde and hydrochloric acid. The samples were further dried and measured with DSC.<sup>[48]</sup>

**Measurements of the Reversibility:** The PVA hydrogels were prepared with 3 cycles of freeze–thaw, followed by soaking in 1.5 M Na<sub>2</sub>SO<sub>4</sub> for 24 h and in 2 M Fe(NO<sub>3</sub>)<sub>3</sub> for 100 min, respectively. The soaking processes were repeated for different cycles and the mechanical properties were measured.

**Dynamically Tuning PVA Hydrogel:** The PVA hydrogel freeze–thawed for three cycles was first immersed in a 1 M Na<sub>2</sub>SO<sub>4</sub> solution for 24 h; then it was washed with plenty of water to remove the salts in the hydrogel. Afterward, the hydrogel was soaked in a 3 M CaCl<sub>2</sub> solution for 48 h. During this soaking process, the images were taken with a camera.

**Fabrication of Brain-Tissue-Mimicking Hydrogels and Softening of the Probe:** To make a brain-tissue-mimicking hydrogel, 100 mL precursor solution was prepared containing 5g monomer acrylamide, 400 mg cross-linker N,N'-methylenebisacrylamide, and 10 μL initiator 2-hydroxy-2-methylpropiophenone. Then the precursor was cured in a cubic mold with UV illumination or printed. To observe the softening process of the probe, a brain-tissue-mimicking hydrogel was first soaked in 2 M

Fe(NO<sub>3</sub>)<sub>3</sub> to exchange the solution in the polymer matrix. Afterward, a hydrogel probe was inserted into the brain-tissue-mimicking hydrogel and they were immersed together in 2 M Fe(NO<sub>3</sub>)<sub>3</sub>.

## Supporting Information

Supporting Information is available from the Wiley Online Library or from the author.

## Acknowledgements

This research used resources of the Advanced Photon Source, a U.S. Department of Energy (DOE) Office of Science User Facility, operated for the DOE Office of Science by Argonne National Laboratory under Contract No. DE-AC02-06CH11357. This research was supported by NSF CAREER Award No. 1724526, AFOSR Award Nos. FA9550-17-1-0311, FA9550-18-1-0449 and FA9550-20-1-0344, and ONR Award Nos. N000141712117 and N00014-18-1-2314.

## Conflict of Interest

The authors declare no conflict of interest.

## Author Contributions

S.W., M.H., and X.H. conceived the concept. X.Z. and X.H. supervised the project. S.W. and M.H., conducted the experiments. J.S. and H.Z. helped with the SAXS measurements. S.W., M.H., and X.H. wrote the manuscript. All authors contributed to the analysis and discussion of the data. S.W. and M.H. contributed equally to this work.

## Data Availability Statement

The data that support the findings of this study are available from the corresponding author upon reasonable request.

## Keywords

Hofmeister effect, ions, poly(vinyl alcohol), tough hydrogels, tunable mechanical properties

Received: November 17, 2020

Revised: December 28, 2020

Published online:

- [1] K. Y. Lee, D. J. Mooney, *Chem. Rev.* **2001**, *101*, 1869.
- [2] J. Li, D. J. Mooney, *Nat. Rev. Mater.* **2016**, *1*, 16071.
- [3] Y. Liu, J. Liu, S. Chen, T. Lei, Y. Kim, S. Niu, H. Wang, X. Wang, A. M. Foudeh, J. B. H. Tok, Z. Bao, *Nat. Biomed. Eng.* **2019**, *3*, 58.
- [4] Y. Huang, M. Zhong, F. Shi, X. Liu, Z. Tang, Y. Wang, Y. Huang, H. Hou, X. Xie, C. Zhi, *Angew. Chem., Int. Ed.* **2017**, *56*, 9141.
- [5] X. Yao, J. Liu, C. Yang, X. Yang, J. Wei, Y. Xia, X. Gong, Z. Suo, *Adv. Mater.* **2019**, *31*, 1903062.
- [6] H. Yuk, T. Zhang, S. Lin, G. A. Parada, X. Zhao, *Nat. Mater.* **2016**, *15*, 190.
- [7] H. Yuk, S. Lin, C. Ma, M. Takaffoli, N. X. Fang, X. Zhao, *Nat. Commun.* **2017**, *8*, 14230.

- [8] J. Y. Sun, X. Zhao, W. R. K. Illeperuma, O. Chaudhuri, K. H. Oh, D. J. Mooney, J. J. Vlassak, Z. Suo, *Nature* **2012**, *489*, 133.
- [9] L. Han, X. Lu, K. Liu, K. Wang, L. Fang, L. T. Weng, H. Zhang, Y. Tang, F. Ren, C. Zhao, G. Sun, R. Liang, Z. Li, *ACS Nano* **2017**, *11*, 2561.
- [10] S. Lin, J. Liu, X. Liu, X. Zhao, *Proc. Natl. Acad. Sci. USA* **2019**, *116*, 10244.
- [11] X. Zhao, *Soft Matter* **2014**, *10*, 672.
- [12] H. Fan, J. P. Gong, *Macromolecules* **2020**, *53*, 2769.
- [13] A. Kumar, S. S. Han, *Int. J. Polym. Mater. Polym. Biomater.* **2017**, *66*, 159.
- [14] O. Chaudhuri, L. Gu, D. Klumpers, M. Darnell, S. A. Bencherif, J. C. Weaver, N. Huebsch, H. P. Lee, E. Lippens, G. N. Duda, D. J. Mooney, *Nat. Mater.* **2016**, *15*, 326.
- [15] A. S. Mao, J. W. Shin, D. J. Mooney, *Biomaterials* **2016**, *98*, 184.
- [16] F. Trenszt, F. Lucien, V. Couture, T. Söllrard, G. Drouin, A. J. Rouleau, M. Grandbois, G. Lacraz, G. Grenier, *Skelet. Muscle* **2015**, *5*, 31.
- [17] W. J. Hadden, J. L. Young, A. W. Holle, M. L. McFetridge, D. Y. Kim, P. Wijesinghe, H. Taylor-Weiner, J. H. Wen, A. R. Lee, K. Bieback, B. N. Vo, D. D. Sampson, B. F. Kennedy, J. P. Spatz, A. J. Engler, Y. S. Cho, *Proc. Natl. Acad. Sci. USA* **2017**, *114*, 5647.
- [18] J. Li, D. Han, Y. P. Zhao, *Sci. Rep.* **2014**, *4*, 3910.
- [19] J. Lee, O. Jeon, M. Kong, A. A. Abdeen, J. Shin, H. N. Lee, Y. Bin Lee, W. Sun, P. Bandaru, D. S. Alt, K. Lee, H. Kim, S. J. Lee, S. Chaterji, S. R. Shin, **2020**, *6*, eaaz5913.
- [20] J. Blacklock, A. Vetter, A. Lankenau, D. Oupický, H. Möhwald, *Biomaterials* **2010**, *31*, 7167.
- [21] I. Hopp, A. Micheltore, L. E. Smith, D. E. Robinson, A. Bachhuka, A. Mierczynska, K. Vasilev, *Biomaterials* **2013**, *34*, 5070.
- [22] S. K. Seidlits, Z. Z. Khaing, R. R. Petersen, J. D. Nickels, J. E. Vanscoy, J. B. Shear, C. E. Schmidt, *Biomaterials* **2010**, *31*, 3930.
- [23] J. R. Capadona, K. Shanmuganathan, D. J. Tyler, S. J. Rowan, C. Weder, *Science* **2008**, *319*, 1370.
- [24] Y. Qiu, E. Askounis, F. Guan, Z. Peng, W. Xiao, Q. Pei, *ACS Appl. Polym. Mater.* **2020**, *2*, 2008.
- [25] J. M. Korde, B. Kandasubramanian, *Chem. Eng. J.* **2020**, *379*, 122430.
- [26] P. Jungwirth, P. S. Cremer, *Nat. Chem.* **2014**, *6*, 261.
- [27] S. Wu, C. Zhu, Z. He, H. Xue, Q. Fan, Y. Song, J. S. Francisco, X. C. Zeng, J. Wang, *Nat. Commun.* **2017**, *8*, 15154.
- [28] R. Du, Y. Hu, R. Hübner, J. O. Joswig, X. Fan, K. Schneider, A. Eychmüller, *Sci. Adv.* **2019**, *5*, eaaw4590.
- [29] L. M. Pegram, M. T. Record, *J. Phys. Chem. B* **2007**, *111*, 5411.
- [30] Y. Zhang, P. S. Cremer, *Curr. Opin. Chem. Biol.* **2006**, *10*, 658.
- [31] R. S. Carnegie, C. L. D. Gibb, B. C. Gibb, *Angew. Chem., Int. Ed.* **2014**, *53*, 11498.
- [32] Y. Yang, X. Wang, F. Yang, H. Shen, D. Wu, *Adv. Mater.* **2016**, *28*, 7178.
- [33] Q. He, Y. Huang, S. Wang, *Adv. Funct. Mater.* **2018**, *28*, 1705069.
- [34] Y. Zhang, S. Furyk, D. E. Bergbreiter, P. S. Cremer, *J. Am. Chem. Soc.* **2005**, *127*, 14505.
- [35] J. Wei, Q. Wang, *Small Methods* **2019**, *3*, 1900558.
- [36] M. Jaspers, A. E. Rowan, P. H. J. Kouwer, *Adv. Funct. Mater.* **2015**, *25*, 6503.
- [37] J. Wang, M. Satoh, *Polymer* **2009**, *50*, 3680.
- [38] A. M. Handorf, Y. Zhou, M. A. Halanski, W. J. Li, *Organogenesis* **2015**, *11*, 1.
- [39] H. Muta, M. Miwa, M. Satoh, *Polymer* **2001**, *42*, 6313.
- [40] P. Lo Nostro, B. W. Ninham, *Chem. Rev.* **2012**, *112*, 2286.
- [41] M. T. I. Mredha, Y. Z. Guo, T. Nonoyama, T. Nakajima, T. Kurokawa, J. P. Gong, *Adv. Mater.* **2018**, *30*, 1704937.
- [42] G. Qu, Y. Li, Y. Yu, Y. Huang, W. Zhang, H. Zhang, Z. Liu, T. Kong, *Angew. Chem.* **2019**, *131*, 11067.
- [43] X. Hu, M. Vatankhah-Varnoosfaderani, J. Zhou, Q. Li, S. S. Sheiko, *Adv. Mater.* **2015**, *27*, 6899.
- [44] J. Liu, H. Zheng, P. S. P. Poh, H. G. Machens, A. F. Schilling, *Int. J. Mol. Sci.* **2015**, *16*, 15997.
- [45] P. Lin, S. Ma, X. Wang, F. Zhou, *Adv. Mater.* **2015**, *27*, 2054.
- [46] P. Lin, T. Zhang, X. Wang, B. Yu, F. Zhou, *Small* **2016**, *12*, 4386.
- [47] Z. Jiang, *J. Appl. Crystallogr.* **2015**, *48*, 917.
- [48] S. Lin, X. Liu, J. Liu, H. Yuk, H.-C. Loh, G. A. Parada, C. Settens, J. Song, A. Masic, G. H. McKinley, *Sci. Adv.* **2019**, *5*, eaau8528.